

# Preparation and characterization of $\text{Ln}_{0.8}\text{Sr}_{0.2}\text{Fe}_{0.8}\text{Co}_{0.2}\text{O}_{3-x}$ (Ln = La, Pr, Nd, Sm, Eu, Gd)

F. Riza <sup>a,\*</sup>, Ch. Ftikos <sup>a</sup>, F. Tietz <sup>b</sup>, W. Fischer <sup>b</sup>

<sup>a</sup>Laboratory of Inorganic Materials Technology, Department of Chemical Engineering, National Technical University of Athens, 157.73 Zografou, Greece

<sup>b</sup>Forschungszentrum Jülich GmbH, Institute for Materials and Processes in Energy Systems, 52425 Jülich, Germany

Received 4 September 2000; received in revised form 23 November 2000; accepted 15 December 2000

## Abstract

In the present study the oxides  $\text{Ln}_{0.8}\text{Sr}_{0.2}\text{Fe}_{0.8}\text{Co}_{0.2}\text{O}_{3-x}$  (Ln = La, Pr, Nd, Sm, Eu, Gd) were prepared and characterized to study the influence of the host rare earth cation on their properties and their potential application as intermediate temperature solid oxide fuel cell cathodes with higher ionic conductivity, lower linear thermal expansion coefficient and better chemical compatibility with the electrolyte. The oxides were prepared by the amorphous citrate synthesis. From X-ray powder diffraction measurements it was deduced that all oxides were single-phased with the sensitivity of the method. However, irregularities during thermal expansion measurements indicated that some structural changes might occur during heating. Only after examination of the powders in a scanning electron microscope, the presence of a second phase (cobalt oxide) in most compositions became evident. © 2001 Elsevier Science Ltd.

**Keywords:** Electrical conductivity; Electron microscopy; Perovskites; Thermal expansion

## 1. Introduction

Over the past years a continuous effort has been made, aiming at better material properties for solid oxide fuel cell (SOFC) components. As far as the cathode is concerned, some of the main aims are to achieve high electronic conductivity, to overcome disadvantages such as chemical reactivity and thermal expansion coefficient (TEC) mismatch with the yttria-stabilized zirconia solid electrolyte and to raise the cathode's catalytic activity for oxygen molecule dissociation and oxygen reduction.<sup>1</sup> Mixed ionic-electronic conductors are considered promising materials. Strontium-doped lanthanum cobaltites are known to possess high electronic conductivity, while iron substitution for cobalt improves significantly their thermochemical and mechanical properties.<sup>2</sup> Strontium doping should not be very high in order to avoid the formation of reaction products with the electrolyte<sup>3</sup> and the TEC increase. Replacing lanthanum cations by heavier rare earth elements also results in less reactive materials

towards the electrolyte material<sup>3,4</sup> with better catalytic activity<sup>5,6</sup> and lower overpotential values.<sup>4</sup>

In an attempt to combine most of the above properties  $\text{Ln}_{0.8}\text{Sr}_{0.2}\text{Fe}_{0.8}\text{Co}_{0.2}\text{O}_3$  oxides, with Ln = La, Pr, Nd, Sm, Eu and Gd, were prepared and characterized.

## 2. Experimental

The oxides were prepared by the amorphous citrate synthesis. Reagents were dissolved in distilled water or nitric acid, mixed and heated over a burner flame until combustion took place and all the mixture got burned. The powder was calcined at 1100°C for 15 h and then milled with zirconia balls in acetone for 24 h. Finally, rectangular rods were formed, pressed at 90 MPa and sintered at 1300°C for 30 h at a 1 K/min heating and cooling rate.

All oxides were characterized by X-ray powder diffractometry (XRD) at room temperature on a Siemens D5000 diffractometer, in the Bragg angle range  $10^\circ \leq 2\theta \leq 80^\circ$ . Further examination of the materials structure was performed with a LEO 1530 scanning electron microscope (SEM) on powder samples sintered at 1200°C for 24 h. Thermal expansion measurements were conducted in air with a DIL 402E Netzsch dilatometer, between 20

\* Corresponding author. Tel.: +301-772-3245; fax: +301-772-3244.

E-mail address: feriza@central.ntua.gr (F. Riza).

and 1100°C (heating/cooling rate: 1 K/min). Electrical conductivity was measured in air with the four point DC method between 20 and 1000°C (heating rate: 5 K/min).

### 3. Results and discussion

XRD measurements at room temperature produced clear patterns for the first three oxides (Ln = La, Pr, Nd) (Fig. 1). For Ln = La the perovskite had a rhombohedral structure, while for Ln = Pr and Nd an orthorhombic structure was observed. Tai et al.<sup>7</sup> report that  $\text{La}_{0.8}\text{Sr}_{0.2}\text{Fe}_{0.8}\text{Co}_{0.2}\text{O}_3$  is orthorhombic, their investigations showed however, that this composition lies directly at the point where the structure changes from the orthorhombic to the rhombohedral unit cell: for iron content up to 70 mol% the perovskite is rhombohedral, while for 80–100 mol% orthorhombic. Moreover, in the next paper of Tai et al.,<sup>8</sup> where the influence of strontium substitution is studied, we see that compounds with Sr-content up to 10 mol% were found to crystallize in the orthorhombic structure whereas compositions with 30–40 mol% in the rhombohedral structure. Thus a small stoichiometric deviation of strontium and/or iron content could lead to the formation of the rhombohedral structure.

The XRD patterns for the last three members (Ln = Sm, Eu, Gd) were rather ambiguous (Fig. 2). After a careful analysis considering various perovskite powder patterns in the ICDD data base (e.g.  $\text{La}_{0.8}\text{Sr}_{0.2}\text{FeO}_3$  ICDD: 35-1480,  $\text{LaFeO}_3$  ICDD: 15-0148), it was assumed that the three compositions were single-phased,

since they matched very well with the  $\text{FeSmO}_3$  structure (ICDD: 39-1490). Dilatometric measurements (Fig. 3) showed that thermal expansion was linear up to 800°C for all oxides. Pr and Nd oxides were proved to possess TECs compatible with the currently used and under study electrolytes (Table 1). However, these thermal expansion curves presented some irregularities at about 900°C, which were most pronounced for the Nd and Eu compounds and made evident that some ordering phenomena took place during heating and cooling in the range of 750–1000°C. Initially it was assumed that a phase transition<sup>7,8</sup> might be the reason for these irregularities and further study with high temperature XRD (HT-XRD) was needed to make clear the reason of these phenomena. HT-XRD measurements made soon evident that no changes in the reflection pattern occurred apart from reversible intensity changes during heating and cooling between 750 and 1000°C. Presumably defect compensation due to oxygen losses during heating<sup>7–9</sup> and/or an isostructural atomic re-ordering took place. Also, a magnetic order  $\leftrightarrow$  disorder transition has to be considered as such transition can affect the thermal expansion of solids, e.g. in the case of NiO.<sup>10</sup> Because a magnetic study of these materials was out of the scope of our work, sintered powder of all six samples was examined with scanning electron microscopy.

For each sample secondary and backscattered electron micrographs were collected. Secondary electron images provide information about the surface morphology, while backscattered electron images in composite contrast show differences in the mean atomic number. The mere fact, that powders instead of a mounted and polished disc

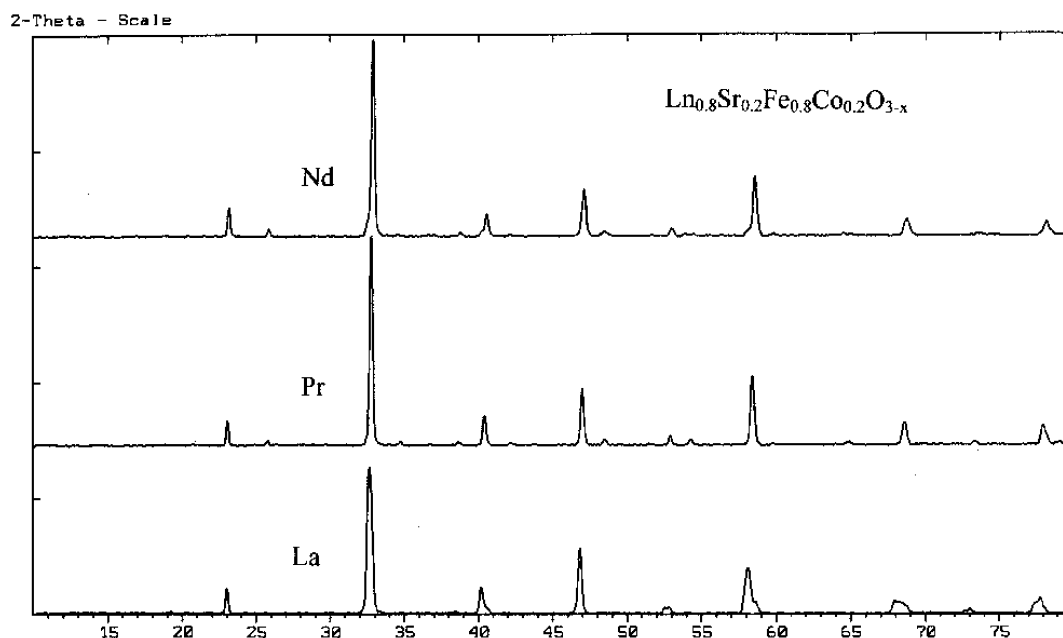


Fig. 1. X-ray powder diffraction patterns of  $\text{Ln}_{0.8}\text{Sr}_{0.2}\text{Fe}_{0.8}\text{Co}_{0.2}\text{O}_{3-x}$ , for Ln = La, Pr, Nd.

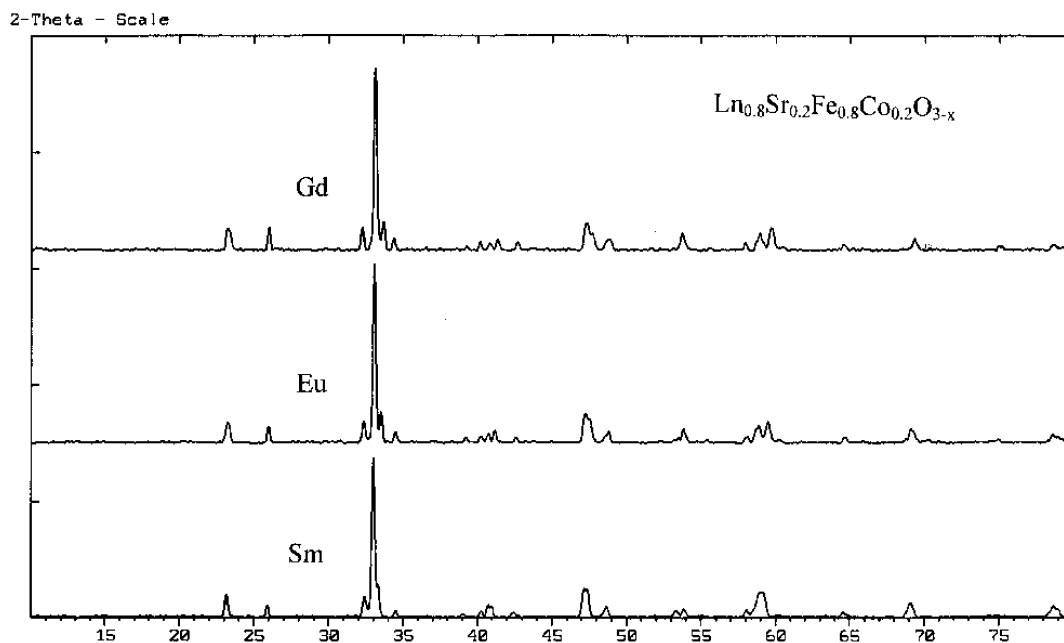


Fig. 2. X-ray powder diffraction patterns of  $\text{Ln}_{0.8}\text{Sr}_{0.2}\text{Fe}_{0.8}\text{Co}_{0.2}\text{O}_{3-x}$ , for  $\text{Ln} = \text{Sm}, \text{Eu}, \text{Gd}$ .

were examined, caused difficulties in the interpretation of the SEM images. Despite this, by comparing secondary with backscattered electron images, we observed that the difference in the mean atomic number was so intense (Figs. 4–7), that it was obvious, that for members with

$\text{Ln} = \text{Sm}, \text{Eu}$  and  $\text{Gd}$ , a second phase existed which was confirmed by EDS analysis on grey and white regions on the particles. By re-examining the XRD patterns, the presence of cobalt oxide ( $\text{CoO}$ , ICDD: 9-0402) was confirmed. The presence of  $\text{CoO}$  (pointed grey areas on micrographs) was barely detectable for the  $\text{Nd}$  perovskite (Fig. 4), while for the  $\text{Sm}, \text{Eu}$  and  $\text{Gd}$  oxides (Figs. 5–7) it became more and more evident. For  $\text{La}$  and  $\text{Pr}$  containing oxides, some evidence for phase impurities can be attributed with certainty either to small stoichiometric deviations or to the influence of surface irregularities. It was thus deduced, that as the rare-earth ionic radius decreases

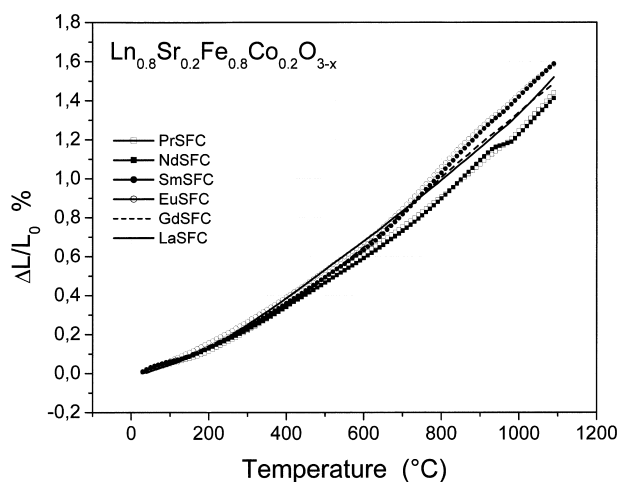


Fig. 3. Thermal expansion curves for  $\text{Ln}_{0.8}\text{Sr}_{0.2}\text{Fe}_{0.8}\text{Co}_{0.2}\text{O}_{3-x}$ , ( $\text{Ln} = \text{La}, \text{Pr}, \text{Nd}, \text{Sm}, \text{Eu}, \text{Gd}$ ) in air.

Table 1  
Specific conductivity and TEC values at 700°C of  $\text{Ln}_{0.8}\text{Sr}_{0.2}\text{Fe}_{0.8}\text{Co}_{0.2}\text{O}_{3-x}$  oxides

$\text{Ln}$	$\sigma_{700} (\text{S cm}^{-1})$	$\text{TEC}_{700} 10^{-6} (^\circ\text{C}^{-1})$
La	179	12.45
Pr	159	11.25
Nd	123	10.91

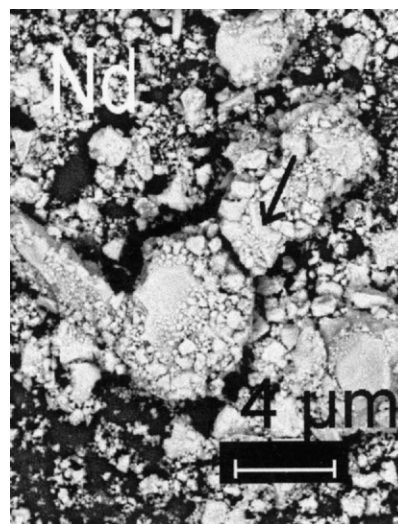


Fig. 4. Backscattered electron micrograph of  $\text{Nd}_{0.8}\text{Sr}_{0.2}\text{Fe}_{0.8}\text{Co}_{0.2}\text{O}_{3-x}$ . Pointed grey areas indicate the presence of  $\text{CoO}$ .

(heavier elements) a miscibility gap exists: a Sr-rich and a Sr-poor phase is formed and a stable solution for strontium does not appear.

Lattice parameters and theoretical density were calculated for the first three oxides (Ln = La, Pr, Nd) from the XRD data, using the least squares unit cell refinement program (LSUCR) (Table 2). Silicon was used as an internal standard during XRD measurements. Density was measured by the Archimedes method. All three compounds were proved to possess at least 97% of their theoretical density.

Electrical conductivity measurements are presented for the perovskites with Ln = La, Pr, Nd. All three compositions showed to possess semiconductive behaviour up to

about 800°C. At this temperature a metal-insulator transition was observed and from then on conductivity decreased with increasing temperature (Fig. 8). Ferrites are known to be substoichiometric in oxygen. The amount of these oxygen vacancies increases with increasing

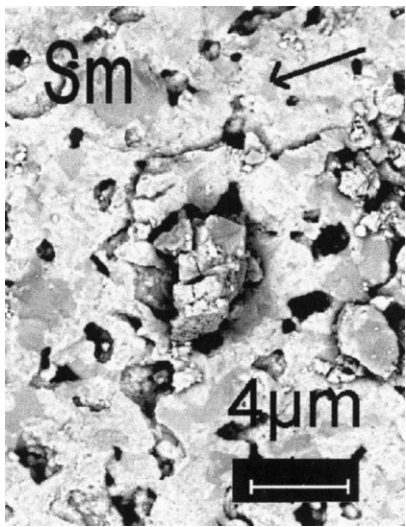


Fig. 5. Backscattered electron micrograph of  $\text{Sm}_{0.8}\text{Sr}_{0.2}\text{Fe}_{0.8}\text{Co}_{0.2}\text{O}_{3-x}$ . Pointed grey areas indicate the presence of CoO.

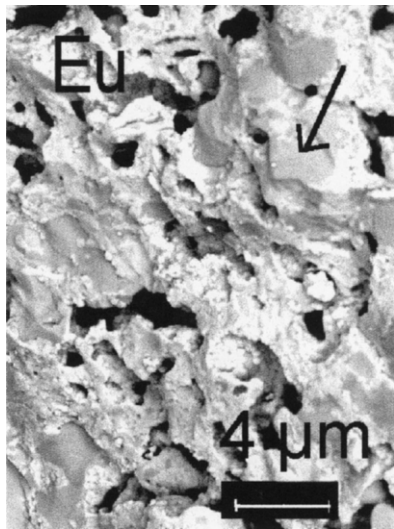


Fig. 6. Backscattered electron micrograph of  $\text{Eu}_{0.8}\text{Sr}_{0.2}\text{Fe}_{0.8}\text{Co}_{0.2}\text{O}_{3-x}$ . Pointed grey areas indicate the presence of CoO.

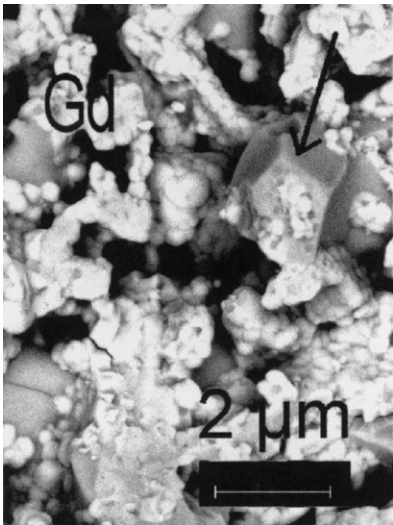


Fig. 7. Backscattered electron micrograph of  $\text{Gd}_{0.8}\text{Sr}_{0.2}\text{Fe}_{0.8}\text{Co}_{0.2}\text{O}_{3-x}$ . Pointed grey areas indicate the presence of CoO.

Table 2  
Structure and lattice parameters of  $\text{Ln}_{0.8}\text{Sr}_{0.2}\text{Fe}_{0.8}\text{Co}_{0.2}\text{O}_{3-x}$  oxides

Ln	Structure	a (Å)	b (Å)	c (Å)
La	Rhombohedral <sup>a</sup>	5.5213	—	13.4134
Pr	Orthorhombic	5.4244	5.4703	7.7214
Nd	Orthorhombic	5.4671	5.5382	7.7410

<sup>a</sup> Hexagonal lattice parameters.

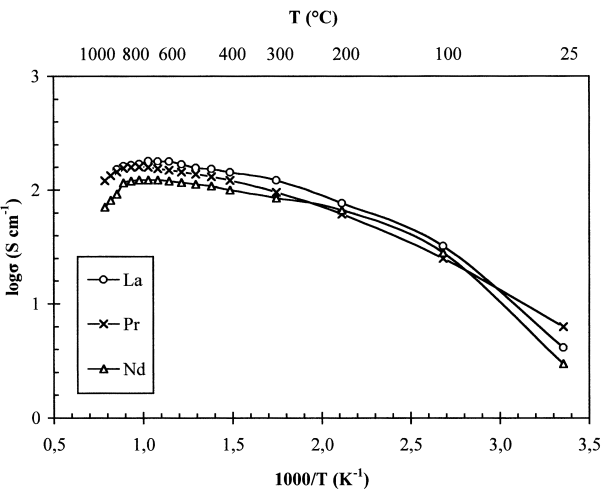
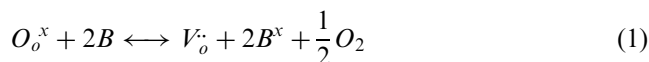


Fig. 8.  $\log \sigma$  versus reciprocal temperature ( $1000/T$ ) for  $\text{Ln}_{0.8}\text{Sr}_{0.2}\text{Fe}_{0.8}\text{Co}_{0.2}\text{O}_{3-x}$ , Ln = La, Pr, Nd.

temperature,<sup>7,8</sup> causing the concentration of the tetra-valent B-ions (Fe, Co) to decrease according to the following equation:



where Kröger–Vink notation is used.

The change in electrical conductivity, i.e. the metal-insulator transition, can on the one hand be due to the continuously changing oxygen content of the samples<sup>11</sup> or, on the other hand, be induced by a magnetic transition as mentioned above since the changes appear in the same temperature region. However, at this stage of the investigations no definite explanation can be given for the reason of the metal-insulator transition.

Nevertheless, the above mentioned compositions (Ln = La, Pr, Nd) meet the requirements for use as intermediate temperature SOFC cathodes ( $\sigma > 100 \text{ S cm}^{-1}$ ) (Table 1).

#### 4. Conclusions

In the Nd compound the second phase, namely cobalt oxide, is just about to appear. From then on it becomes more and more apparent. Dilatometric and electrical conductivity measurements proved that the oxides with Pr and Nd as the host rare earth cation could be taken into consideration as cathode materials for intermediate temperature SOFCs, provided that the Nd oxide acquires a more stable structure.

From HT-XRD and SEM characterization it became obvious that much attention has to be paid at the evaluation of XRD patterns of compositions, that have not been extensively studied and for which structure data are insufficient. Apart from XRD characterization, SEM micrographs should be made, in order to ensure that the materials are actually single-phased. It is definitely

interesting to know, the circumstances, under which the formation of cobalt oxide takes place.

#### References

1. Gellings, P. J. and Bouwmeester, H. J. M., *Handbook of Solid State Electrochemistry*. CRC Press, 1997, pp. 413.
2. Kilner, J., Benson, S., Lane, J. and Waller, D., Ceramic ion conducting membranes for oxygen separation. *Chemistry and Industry*, 1997, 907–911.
3. Kostogloudis, G. Ch. and Ftikos, Ch., Chemical compatibility of  $\text{RE}_{1-x}\text{Sr}_x\text{MnO}_{3\pm\delta}$  (RE = La, Pr, Nd, Gd,  $0 \leq x \leq 0.5$ ) with yttria stabilized zirconia solid electrolyte. *J. Eur. Ceram. Soc.*, 1998, **18**, 1707–1710.
4. Kostogloudis, G. Ch. and Ftikos, Ch., Characterization of  $\text{Nd}_{1-x}\text{Sr}_x\text{MnO}_{3\pm\delta}$  SOFC cathode materials. *J. Eur. Ceram. Soc.*, 1999, **19**, 497–505.
5. Teraoka, Y., Nobunanga, T. and Yamazoe, N., Effect of cation substitution on the oxygen semipermeability of perovskite-type oxides. *Chem. Lett.*, 1988, 503–506.
6. Tu, H. Y., Takeda, Y., Imanishi, N. and Yamamoto, O.,  $\text{Ln}_{0.4}\text{Sr}_{0.6}\text{Co}_{0.8}\text{Fe}_{0.2}\text{O}_{3-\delta}$  (Ln = La, Pr, Nd, Sm, Gd) for the electrode in solid oxide fuel cells. *Solid State Ionics*, 1999, **117**, 277–281.
7. Tai, L.-W., Nasrallah, M. M., Anderson, H. U., Sparlin, D. M. and Sehlin, S. R., Structure and electrical properties of  $\text{La}_{1-x}\text{Sr}_x\text{Co}_{1-y}\text{Fe}_y\text{O}_3$ . Part 1. The system  $\text{La}_{0.8}\text{Sr}_{0.2}\text{Co}_{1-y}\text{Fe}_y\text{O}_3$ . *Solid State Ionics*, 1995, **76**, 259–271.
8. Tai, L.-W., Nasrallah, M. M., Anderson, H. U., Sparlin, D. M. and Sehlin, S. R. Structure and electrical properties of  $\text{La}_{1-x}\text{Sr}_x\text{Co}_{1-y}\text{Fe}_y\text{O}_3$  Part 2. The system  $\text{La}_{1-x}\text{Sr}_x\text{Co}_{0.2}\text{Fe}_{0.8}\text{O}_3$ . *Solid State Ionics*, 1995, **76**, 273–283.
9. Tietz, F., Peculiarities in the thermal expansion behaviour of ceramic fuel cell materials. In *Proc. 9th Int. Conf. on Modern Materials and Technologies (CIMTEC '98)-World Ceramic Congress and Forum on New Materials, Vol. 24. Innovative Materials in Advanced Energy Technologies*, ed. P. Vincenzini. Techna Publishers, Faenza, Italy, 1999, pp. 61–70.
10. Foëx, M., Sur les anomalies de propriétés accompagnant la transformation du type  $\lambda$  du protoxyde de nickel. *Bull. Soc. Chim. France*, 1952, **19**, 373–379.
11. Trofimenko, N. E. and Ullmann, H., Oxygen stoichiometry and mixed ionic-electronic conductivity of  $\text{Sr}_{1-a}\text{Ce}_a\text{Fe}_{1-b}\text{Co}_b\text{O}_{3-x}$  perovskite-type oxides. *J. Eur. Ceram. Soc.*, 2000, **20**, 1241–1250.